Exp Brain Res (1999) 126:1–18

RESEARCH ARTICLE

G.E. Loeb · I.E. Brown · E.J. Cheng

A hierarchical foundation for models of sensorimotor control

Received: 12 February 1998 / Accepted: 2 December 1998

Abstract Successful performance of a sensorimotor task arises from the interaction of descending commands from the brain with the intrinsic properties of the lower levels of the sensorimotor system, including the dynamic mechanical properties of muscle, the natural coordinates of somatosensory receptors, the interneuronal circuitry of the spinal cord, and computational noise in these elements. Engineering models of biological motor control often oversimplify or even ignore these lower levels because they appear to complicate an already difficult problem. We modeled three highly simplified control systems that reflect the essential attributes of the lower levels in three tasks: acquiring a target in the face of random torque-pulse perturbations, optimizing fusimotor gain for the same perturbations, and minimizing postural error versus energy consumption during low- versus high-frequency perturbations. The emergent properties of the lower levels maintained stability in the face of feedback delays, resolved redundancy in over-complete systems, and helped to estimate loads and respond to perturbations. We suggest a general hierarchical approach to modeling sensorimotor systems, which better reflects the real control problem faced by the brain, as a first step toward identifying the actual neurocomputational steps and their anatomical partitioning in the brain.

Key words Motor control · Modeling · Spinal cord · Muscles · Muscle spindles · Reflexes · Neural networks

Introduction

Theories of sensorimotor control based on engineering control theory usually break a problem into a series of transformations (e.g., coordinate transformations, inverse kinematics, inverse dynamics, etc.). In order to apply such theories to living organisms, it is necessary to identify the locus of each of these transformations and the nature of the computational machinery that performs them. This has proven to be difficult (Imamizu et al. 1995). In this paper, we explore the types of behavior and control strategies that emerge in model systems whose components have biologically relevant input-output relationships and connectivity:

1. Biological muscles differ from robotic torque motors in that they produce large, instantaneous changes in output force when kinematic conditions change (recently modeled by Brown et al. 1996), but respond only sluggishly when neural activation changes.
2. Biological feedback circuits differ from robotic servocontrollers in that they have few "private-line" paths whereby command or feedback signals can be routed selectively to individual actuators. Instead, the signals from large numbers of noisy sensors of diverse physical variables converge with the signals from many command centers before they are routed to motoneurons.
3. Biological performance differs from that of industrial robots in that animals usually find it more valuable to perform suboptimally, but adequately in the widest possible range of circumstances rather than to perform optimally, but only for nominal conditions.

The above three attributes can each be associated with one level of an essentially hierarchical system, with the musculoskeletal plant itself at the bottom, the spinal cord in the middle, and the brain at the top. Researchers tend to confine themselves to one or the other of these subsystems of components and behaviors. Those who study the "adaptive circuitry" at the top usually assume that it bypasses the fixed circuitry of the spinal cord to take direct control of the muscles required to perform learned tasks (Fetz and Shupe 1990). Modellers of control systems often pay little attention to the properties of the sensors and actuators actually available, assuming that these should and can be converted to simple state variables, such as end-effector position, joint angles, veloci-

G.E. Loeb (✉) · I.E. Brown · E.J. Cheng
MRC Group in Sensory-Motor Neuroscience, Abramsky Hall, Queen's University, Kingston, ON K7L 3N6 Canada
e-mail: loeb@biomed.queensu.ca
Tel.: +1-613-533-2790, Fax: +1-613-533-6802

ty, and force by computational processes known as coordinate transformations (Soechting and Flanders 1992).

This article considers some of the functional relationships that might be expected among the brain, spinal cord, and sensorimotor apparatus as a consequence of the known structure, function, and phylogeny of each. Because these levels must work synergistically in the performance of most behaviors, a knowledge of the strengths and limitations of each level should facilitate the schematization of the overall problem of sensorimotor control into a set of modules that have some likelihood of one-to-one correspondence with actual biological structures. Such knowledge is also necessary for the interpretation of experimental data, which usually involves inferences about how activity in one structure contributes to the observed behavior based on assumptions about signals and variables that cannot be recorded directly. Previous modeling work has focused on developing realistic models of complete neuromusculoskeletal systems (e.g. He et al. 1991; Bullock and Grossberg 1992), but it is difficult to appreciate the relative contributions of individual elements and connections in their myriad details. The present work explores the surprisingly sophisticated emergent properties that arise even in extremely simple models when they incorporate realistic operating conditions and hierarchical structure.

Principles

The value of hierarchical structure

Hierarchical models of nervous-system function have lost favor as new methods for tracing circuitry and mapping functional activity have revealed widespread ascending, descending, and recurrent loops involving most areas of the brain. For the cognitive systems that provide most of these data, strictly hierarchical processing is undesirable because it would decrease the ability of the brain to interpret complex situations involving contextual clues. Motor systems, however, are judged at least as much on speed as on accuracy. They must delegate at least a portion of the decision-making to lower centers, much as a modern army distributes standing orders and contingency plans to front-line units that first encounter situations in which an immediate response is imperative. These units lack the overall contextual information required to reformulate objectives or strategies, but they can interpret incoming data and execute tactical responses according to their standing orders. Obviously, the higher command centers must anticipate the actions of the front-line units, must be able to develop and transmit new standing orders to fit each new situation, and must be able to countermand old standing orders when they appear to be missing the objective.

The main divisions of the hierarchy

This study considers three levels of the sensorimotor hierarchy and the nature of the information transmitted between them. At the bottom is the musculoskeletal plant itself, whose many sensors and actuators have complex intrinsic properties, which are determined both by their physical form and by their postural deployment and activation by the central nervous system. The next level is the spinal cord, a primitive, but powerful machine for rapid tactical responses to a wide range of inputs. These first two are the “lower levels” that are the main subject of this paper. At the top is the brain, which we have subdivided loosely into two subcomponents for posing objectives and developing strategy. We have not attempted to identify these functional subdivisions with anatomical subdivisions of brain motor function (e.g., cerebral cortex, cerebellum, basal ganglia). Such putative assignments and further subdivisions of motor planning depend upon explicit or implicit assumptions about the properties and capabilities of the lower levels of such a hierarchy.

The role of perturbations

Every motor task has associated with it a particular set of perturbations, which may be external and/or internal to the organism. External mechanical perturbations may be applied explicitly by an investigator or they may be associated implicitly with external objects and circumstances that are part of the task. Even without overt mechanical perturbations, internal perturbations arise inevitably from noise in the neural processes of initiating all-or-none action potentials and integrating them asynchronously and often nonlinearly, for example from sensors (Stein 1965; Loeb and Marks 1985), in motoneurons (Matthews 1996), and in the movement-planning centers themselves (Bullock and Contreras-Vidal 1993). The probability of these perturbations influences the tactics that an adaptive controller such as the brain adopts. In the absence of perturbations, many different sets of tactics may be functionally equivalent, a problem that motor psychologists describe as motor redundancy or overcompleteness (Bernstein 1967). Theoreticians attempt to deal with this problem by “optimizing” control strategies for global performance criteria, which are defined not by the task, but instead are assumed to be fixed for the organism, such as minimizing energy consumption or mechanical stress on joints (Davy and Audu 1987; Collins 1995). In our models, external perturbations and internal computational noise provide a means for distinguishing and selecting between otherwise equivalent strategies on the basis of the explicit performance criteria for the task itself (Brown and Loeb 1999).

The use of intrinsic coordinate representations

Theories of motor planning from a “top-down” perspective usually employ an orthogonal coordinate frame in which to represent the goals of the task, typically in Cartesian coordinates with the origin at a particular body part, such as the eyes, head, trunk, or shoulder (Buneo et al.

1995; Soechting and Flanders 1992). Much of the motor-planning task then consists of transforming the desired trajectory from this coordinate frame into the non-orthogonal coordinate frame of individual muscles, usually through an intermediate coordinate frame of joint angles (Hollerbach and Atkeson 1987). Somatosensory information is required to define the starting posture of the body and to monitor the progress of the task in order to generate corrections to the concurrent or future instances of the task. Much of this information is derived from proprioceptors operating in the intrinsic coordinates of the muscles in which they reside. The remainder derives from cutaneous receptors, whose location in Cartesion extrapersonal space depends on limb posture, as determined from proprioceptive information. If motor planning is, in fact, conducted in an orthogonal coordinate frame, then there must be an inverse transformation to convert non-orthogonal somatosensory information into a compatible coordinate frame for feedback control and evaluation of performance (Pellionisz 1986; Scott and Loeb 1994).

In our model systems, we have only used the natural coordinate system that arises from the set of sensory receptors themselves. For simplicity, we have identified them with simple physical variables such as length, velocity, and force; what is important is that they sense at the level of the muscle rather than in exteroceptive coordinates, such as the end-point of the limb. This sensory coordinate frame is used by our model brain not only for feedback control, but also to specify motor tasks, to identify loads, and to evaluate and adapt control strategies. MacKay (1982) and Burgess (1992) advocated, but did not develop a similar notion of "sensory templates" in motor planning.

Descending information is substantially transformed by the spinal cord through its interneurons, which receive most of the descending information, combine it with segmental afferent feedback, and direct it to divergent motor nuclei (Lundberg et al. 1987; Schomburg 1990; Jankowska 1992). There is little evidence, however, that this constitutes a general transformation from an orthogonal coordinate frame (such as end-point position, movement vectors, or joint angles) into the intrinsic coordinates of the muscle. It seems more likely that these interneurons reflect the control requirements of primitive behaviors (e.g., postural stability, locomotion, escape) that evolved long before brains began formulating detailed strategies for limb movements (Loeb et al. 1989, 1990). The various types of interneurons that occur in the spinal cord define another important and inherently non-orthogonal intrinsic coordinate frame upon which the brain must operate.

Model system

In order to reveal general emergent properties of the hierarchy, we devised model systems with the fewest numbers of elements that were capable of expressing these properties. This permitted us to explore fully the effects of varying key elements and their parameters and to view graphically the entire performance space of control systems during various tasks. The general design of the model is shown in Fig. 1 in both mathematical and schematic forms. Wherever possible, mechanical parameters were normalized to physiological constants (e.g., muscle-fiber length, maximal isometric force) or dimensionless values in the range ±1; neural signals were treated as continuous and were combined linearly. The kinetic components of the system were modeled in the Working Model software environment (Knowledge Revolution,

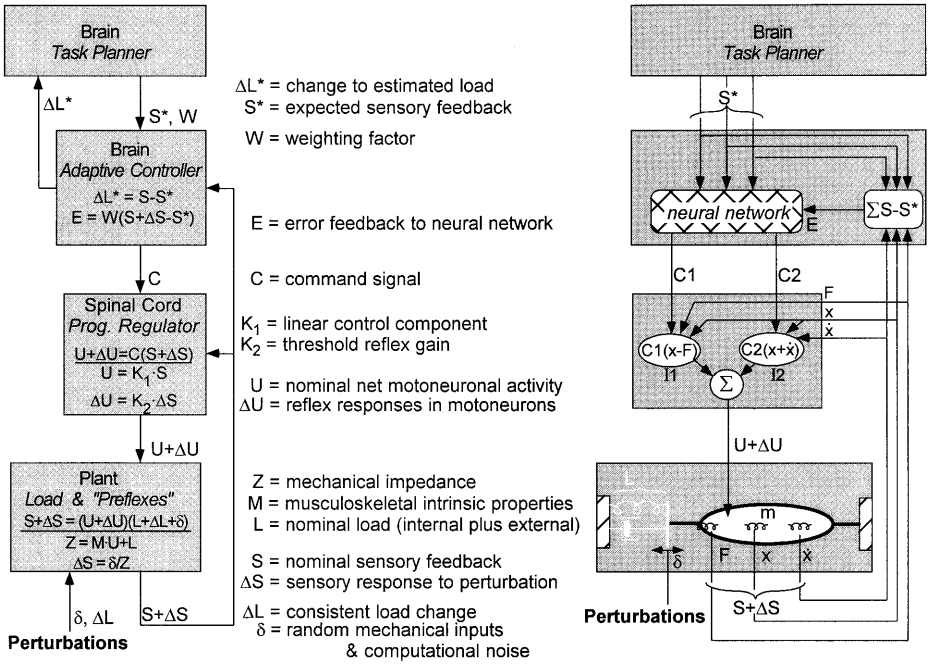

Fig. 1 Hierarchical model system shown in general mathematical form (left), together with a table of symbols used in this article, and a simplified example used for model 1 (right), whose performance is given in Figs. 2, 3, 4

San Mateo, Calif., USA), which was dynamically linked to control models implemented in MATLAB (Math Works Inc., Natick, Mass., USA). The equations and parameters are provided in the Appendix, with a link to a downloadable version of a general muscle model.

Musculoskeletal plant

The models described in this article had only a single degree of freedom operated by one or two muscles. Each muscle was controlled by a single alpha motoneuron, whose level of excitation (U) could vary from 0 to 1. Importantly, the force-generating properties of the muscle were designed to be physiologically realistic (see Appendix), including a low-pass filter for electromechanical activation delay (approximately 80 ms time-constant), nonlinear force-length and force-velocity relationships (Fig. A1, adapted from Brown et al. 1996), and internal mass (required for computational stability when operating against springlike loads; He et al. 1991). The muscle had maximal isometric force-generating ability (F_0) at the starting length of L_0. Each muscle was equipped with two or three sensors (set S), corresponding approximately to the physiological Golgi tendon organ (sensor of stress between muscle and load, F), muscle-spindle secondary ending (sensor of muscle length, x), and muscle-spindle primary ending (sensor of muscle velocity, dx/dt). Various perturbations (δ) could be added to the load during the performance of a task. The response to these perturbations (ΔS) depended on the effective impedance (Z) presented by the load plus intrinsic muscle properties, which in turn depended on the activation level and the force-length and force-velocity properties of the muscle(s).

Programmable regulator

The model of the spinal cord consisted of two or three interneurons (I1, I2,...), each of whose output depended on the product of a corresponding command signal from the brain (C1, C2,...) times the sum of two of the sensor signals. This was intended to simulate the multimodal nature of afferent input to most known spinal interneurons and their biasing by descending projections from higher control systems (Lundberg et al. 1987; Schomburg 1990; Jankowska 1992). The outputs from two interneurons were summed by the alpha motoneuron to generate the extrafusal component of U; in the model with fusimotor control, only one of the interneurons controlled the gamma motoneuron. In the models presented here, the interneurons operated linearly (no threshold or rectification) to modulate both the nominal motor program U and the reflex responses (ΔU) in response to the ongoing sensory input ($S+\Delta S$). In model 1 illustrated in Fig. 1, one interneuron (I1) received excitatory input from the length sensor and inhibitory input from the force sensor, similar to the Ib inhibitory interneuron (Jankowska and McCrea 1983; Jankowska 1992). This pattern of feedback has been called “stiffness regulation” (Houk 1979). The second interneuron (I2) received excitatory inputs from both the velocity and length sensors, a pattern of feedback similar to that described for the combined effects of spindle primary and secondary afferents (Marque et al. 1996). (There is no explicit representation of the Ia monosynaptic projection because its gating by presynaptic inhibition makes this pathway functionally equivalent to the interneuronal representation used here.) Such sets of multimodal feedback gains are called programmable regulators in engineering control theory, where they are used for multi-input-multi-output systems that need to be optimized for different performance criteria at different times (Athans and Falb 1969; Loeb et al. 1990; McIntyre et al. 1996).

Adaptive controller

The control signals that accomplish a given task must be learned by the adaptive controller using a process of trial and error. In the nervous system, this is presumably carried out by a neural network, employing a process akin to gradient descent (Burnod et al. 1992). Our models were deliberately restricted to only two command signals, so that we could graphically represent the entire space of all possible outputs from the controller to the spinal cord and identify globally optimal control strategies. More realistic systems would have many more sensors and interneurons with more complex properties and connectivity, which would likely give rise to multiple local minima.

We specified the task in the same coordinates used to evaluate the performance of the task, namely the intrinsic set of sensory signals (S) available from the musculoskeletal plant. Performance was judged according to the distance of the target state (S^*) from the actual state ($S+\Delta S$) at the specified time, with equal weighting (W) of the errors in all of the intrinsic sensory coordinates. Perturbations consisted of various forces applied at various times during the movement. Performance was judged according to the mean error achieved over all of the predetermined perturbation conditions; note log plots of error used throughout.

Task planner and load estimator

The adaptive controller must be assigned a goal that is achievable. For a given load, only certain conditions in multidimensional space S are possible. The coordinates of space S are the state variables of the system, which we constrain to be identical to whatever sensors are available in the model system. For the first two musculoskeletal systems explored here, these possible conditions lie on a curved surface in a three-dimensional space, depicted in Fig. 2A by the shaded surface. Thus, this surface (L^*) is essentially a model of this load (L), which con-

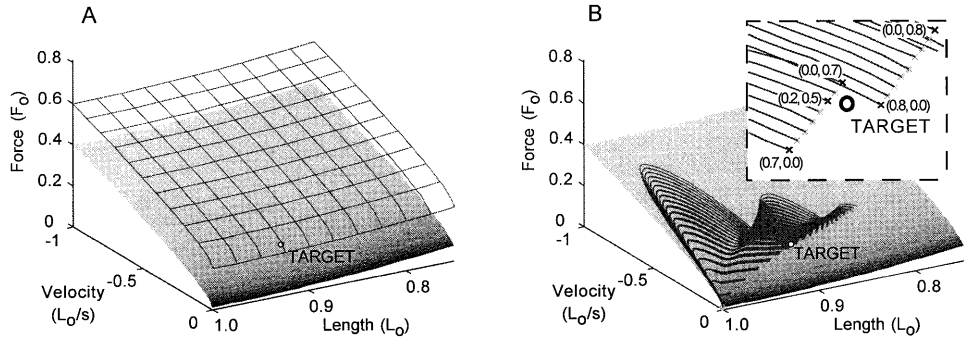

Fig. 2 **A** For the three-sensor model in Fig. 1 (right), all possible states of the system exist in a three-dimensional space with sensor-defined axes of length, velocity, and force. For the nonlinear spring and dashpot loads in this model, the only possible states lie on the shaded, curved surface; adding an additional force-generating element would shift the surface, as indicated by the grid. **B** The family of 0.5-s-long trajectories (*fine lines* with *crosses* at endpoints) for all 121 different step commands to the interneurons (C1, C2) shown in the model of Fig. 1 (right). *Inset* Detail of the trajectories ending near the target region shows the resolution limit of the command steps tested

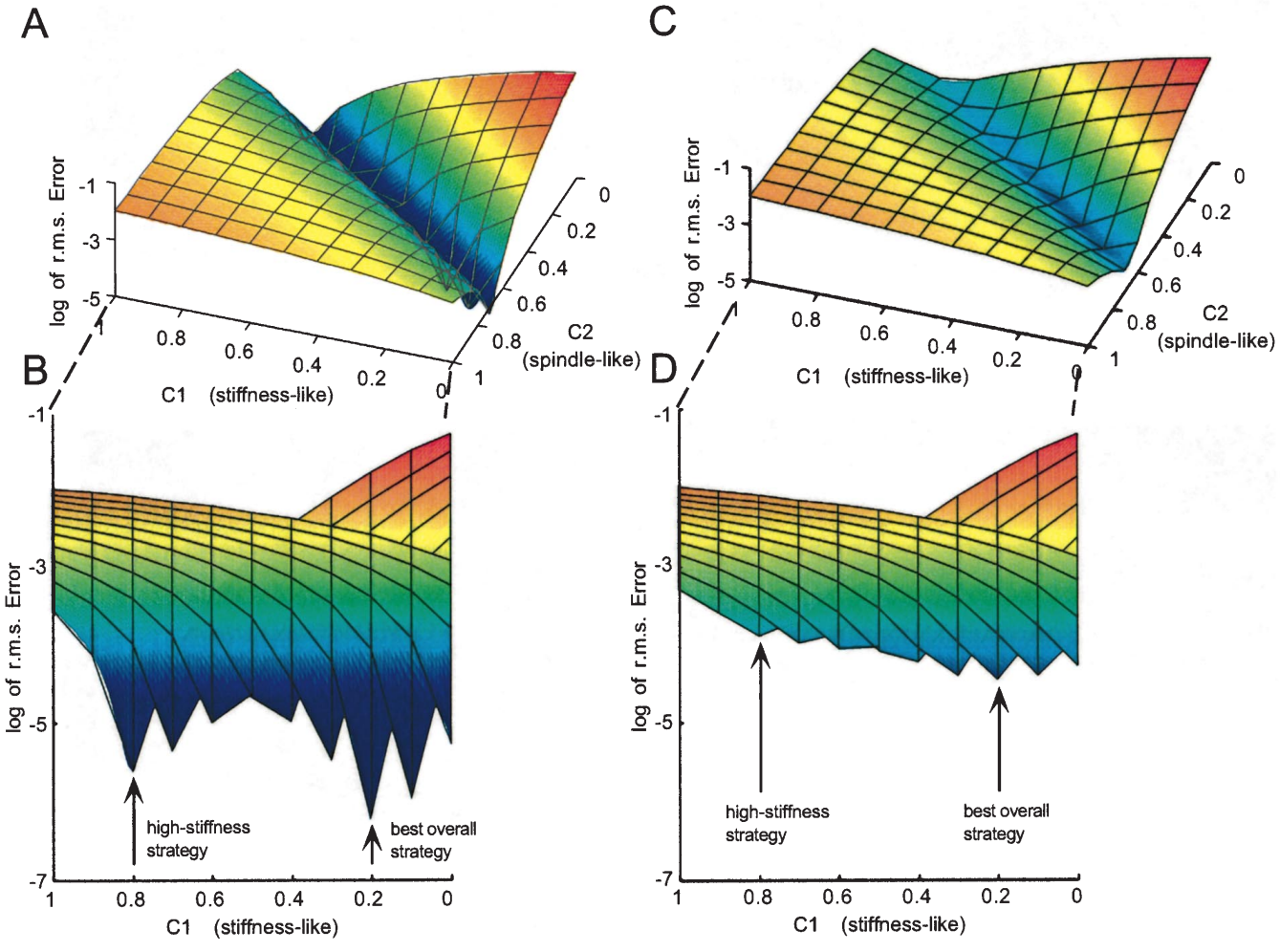

Fig. 3 **A** Plot of distance (error, log of root mean square) on the load surface in state-space between the target and the end of trajectory without perturbations for all control settings (C1, C2). **B** Vertically magnified view from the side, with *arrows* denoting two strategies compared in Fig. 4. **C**, **D** Similar error plots for an average of 12 different perturbation conditions tested for each control setting

sists of a parallel, nonlinear spring and dashpot with zero inertia. Changes in command signals produce trajectories of movement on this state surface. For a different load condition or during a perturbation, the trajectory must lie on a different surface. The grid in Fig. 2A shows a new surface that results when a constant force is added to the musculoskeletal plant, such as might be applied by a constant-tension spring or a torque pulse in a typical experiment on load-compensating ability. As discussed below, persistent deviations between the target S^* and the sensory feedback S actually received indicate that the target S^* does not lie on surface L. Because the coordinate frame for the internal representation of load (L^*) is the same as that for sensory feeback (S), the deviation information can be used directly by the Task Planner to modify this internal representation according to $\Delta L^* = S - S^*$.

Model results

Exploring the control space for a ballistic task (model 1)

The system started at rest with $C1=C2=0$, which results in $U=0$ with the muscle lying at length L_0 where $F=0$ (this condition corresponds to an uncontrolled extreme position in this unbalanced, single-muscle system). The Target was a particular combination of length and velocity to be reached 0.5 s after start, somewhat akin to hitting a baseball. All possible combinations of step changes to commands $C1$ and $C2$ were tested over the range 0–1 in increments of 0.1 for each. This resulted in the family of 0.5 s duration trajectories in sensory state space shown in Fig. 2B. The root-mean-square distance in the state-space (force, length, velocity) from the target to the end-point of each trajectory was plotted as a function of the $C1$ and $C2$ inputs producing that trajectory (Fig. 3A, B). A subset of command strategies ($C1+C2=0.7$ or 0.8) produced essentially equally good results (the fluctuations in the minima seen in the sideways detailed view of Fig. 3B reflect the coarse grain of the C values actually tested rather than any trend, as shown by inset of Fig. 2B).

It is important to note that the nominal muscle activation U produced by these various control programs is time-varying in a different way for each program. This is because U is determined not just by constant input C to each interneuron during the movement, but also by the ongoing, time-varying sensory feedback S to these interneurons. As can be seen in Fig. 4B and D, the nominal trajectory (before the perturbation) associated with the "best overall strategy" produced a lower initial activation of the muscle than another "high-stiffness strategy" with similar results, but these became more similar as the effects of sensory feedback during the movement counteracted the continuing differences in command signals C.

Dealing with random force-pulse perturbations (model 1)

In order to differentiate the effectiveness of the subset of control settings that performed equally well in the nomi-

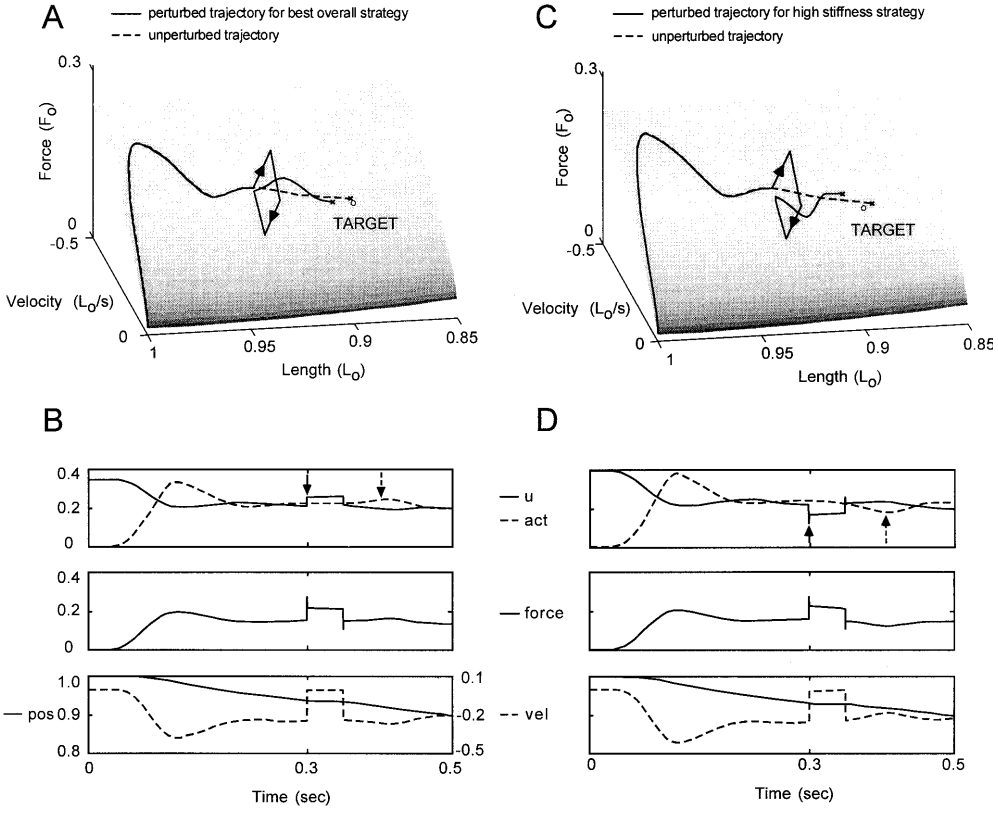

Fig. 4 **A** The trajectories (on the load surface) for the best overall strategy (identified in Fig. 3B, D), shown without and with a 50-ms-long perturbation consisting of +0.2 F_0 at 0.3 s into the trajectory (*arrows* denote vertical shifts between the two surfaces, defining the nominal and perturbed systems, as shown in Fig. 2A). **B** Kinetics [motoneuron excitation (*u*), muscle activation (*act*), and force] and kinematics [velocity (*vel*) and position (*pos*)] versus time for the best overall strategy. **C, D** Corresponding plots for the high-stiffness strategy. Note opposite sign of reflex activity produced by the two strategies (*arrows* in **B** and **D**)

nal condition, we simulated their behavior when the task was performed in the presence of brief (50 ms duration) force perturbations that varied in direction and magnitude (±0.1 and ±0.2 F_0) and time (0.1, 0.2 or 0.3 s after onset of control program). Under these conditions, there was a clear trend (Fig. 3C, D) toward better performance for strategies that used a relatively high value for *C2* (spindle-like excitatory feedback of length and velocity) and low values for *C1* (stiffness servo with excitatory length and inhibitory force feedback). Examples of these strategies with and without a sample perturbation are shown in Fig. 4. The best overall strategy responded to the stretch produced by the positive force pulse with a net excitatory reflex that tended to stabilize the desired trajectory. The high stiffness strategy produced a net inhibitory reflex as a result of the force-feedback, which increased the overall error. The apparent redundancy of control strategies with equally good performance in the unperturbed state could be resolved into a single optimal strategy when the task was performed under conditions that included a set of randomly presented perturbations. We expect, but have not explicitly tested that the application of perturbations of position rather than force would favor the high stiffness strategy because the inhibitory force feedback would then reduce the error in the force dimension.

Fusimotor control (model 2)

A second version of the model was created to examine the effects of fusimotor gain γ on the velocity sensor. The underlying hypothesis was that the inclusion of noise and perturbations in the model system would resolve an apparent redundancy in the motor control system, similar to model 1, but involving fusimotor control with no direct mechanical effect on the task. As shown in Fig.5, changing the fusimotor gain simply changed the slope of the sensor output versus muscle velocity, an effect which, in principle, could be compensated at least partially by changing the gain of the interneuron receiving this sensor's signal (I2). A more useful rationale for fusimotor control is to optimize the signal-to-noise ratio of the available velocity feedback in the face of intrinsic noise in the transducer and limitations in the dynamic range of its output signal (Loeb and Marks 1985; Scott and Loeb 1994). In simulating these processes, the velocity was biased to the target velocity for this model (–0.32 L_0/s) before the gain factor γ was applied, which prevents changes in fusimotor gain from biasing the sensor asymmetrically toward one end of its dynamic range. First, we added band-limited (2–5 Hz) noise to the sensor output, and then we clipped the output (see Appendix, model 2, and Fig. 6). The fusimotor gain itself was controlled by command C1, which also contributed to alpha motoneuron activation, reflecting the general tendency for intra- and extrafusal activity to occur simultaneously (including through common beta motoneurons). It is important to note that this is a highly oversimplified representation of normal spindle function, which includes at least two independently controlled types of fusimotor input with different and more complex effects on both length and velocity sensitivity of primary and secondary spindle afferents (for review, see Loeb 1984).

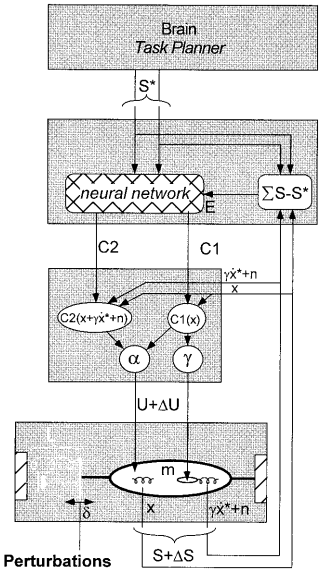

Fig. 5 Schematic design of model 2, used to test fusimotor control strategies. Force sensor omitted and velocity sensor provided with variable gain set by fusimotoneuron γ (after adding fixed bias relative to target velocity) plus added band-limited noise *n*. Symbols otherwise as in Fig. 1

The relative performance of 121 different command settings spanning (0.0, 0.0) to (1.0, 1.0) in steps of 0.1 is shown in Fig. 6. The top graph of each pair shows the signal from the velocity sensor for the command settings that produced the best performance in the final, most realistic condition (Fig. 6D). The bottom graph shows the r.m.s. error for all command settings for the condition indicated, with a red dot indicating the command setting plotted at the top. For each nominal task condition, each value of *C1* had a corresponding (but gradually changing) value of *C2* that produced the best performance, resulting in a diagonal trough in the error plot. In the condition with no perturbations, no sensor noise, and no output clipping (Fig. 6A), almost all of these "best pairs" performed equally well (except for those where the *C2* gain was limited by the range of the simulations). When perturbations alone were added to the load (Figure 6B, average of six trials with 50 ms duration force-pulses of ±0.3 F_0 at 0.1, 0.2, and 0.3 s into the trajectory), a smaller group of approximately equivalent optimal strategies emerged in the middle of the (*C1*, *C2*) range. When noise was added to the velocity sensor in addition to the force perturbations in the load (Fig. 6C), the best performance moved to the higher range of C1. This corresponded to higher fusimotor gain, which increased the overall amplitude of the velocity sensor signal so that the noise was a smaller proportion of the signal. When the amplitude of the velocity sensor output was clipped (Fig. 6D), the best performance shifted back to somewhat lower values of fusimotor gain, in which the sensor spent less time at saturated output levels during the perturbations. Note that the velocity sensor was clipped only for values that exceeded its output range during the optimal

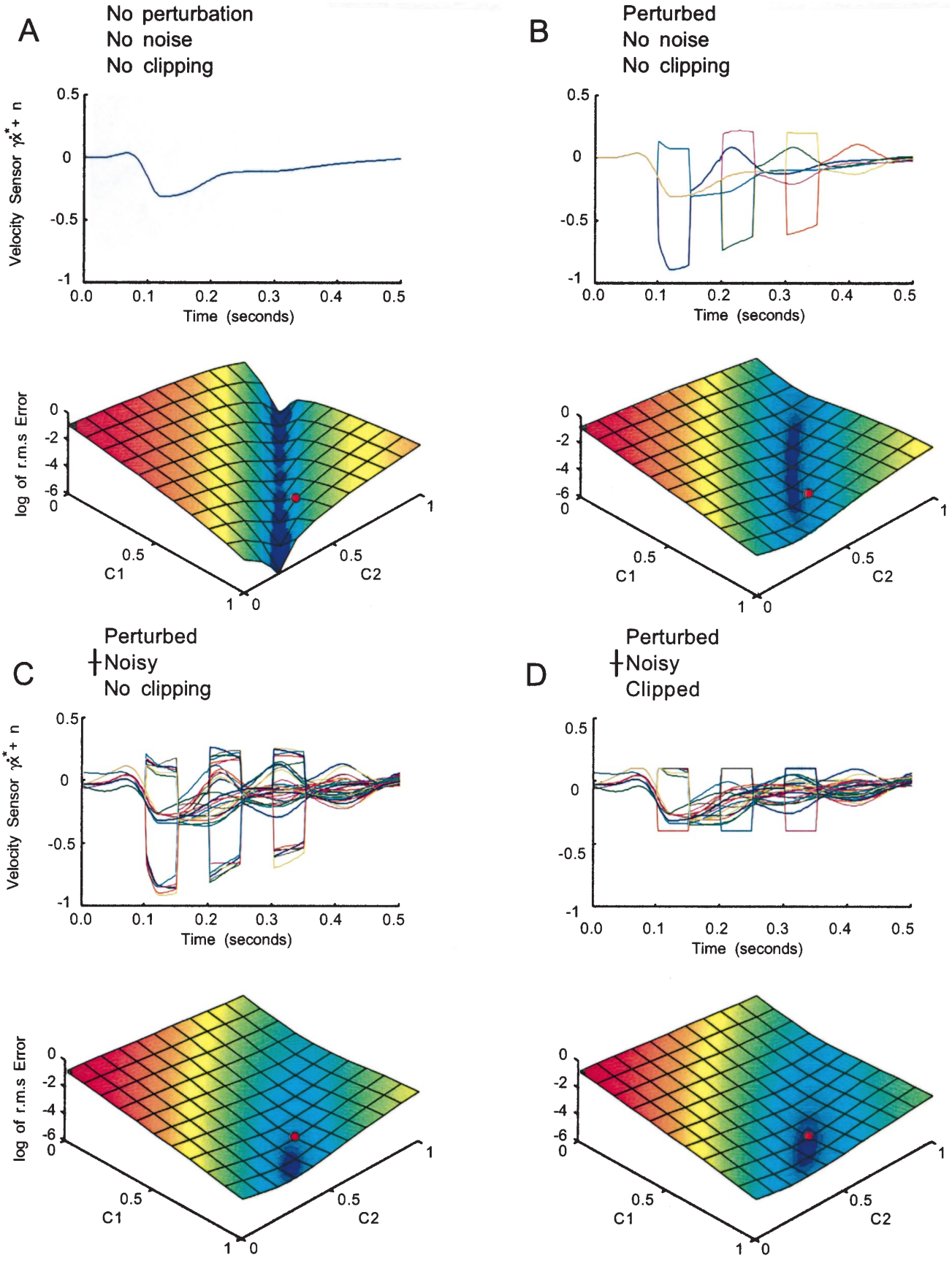
A
No perturbation
No noise
No clipping
B
Perturbed
No noise
No clipping
C
Perturbed
Noisy
No clipping
D
Perturbed
Noisy
Clipped
Velocity Sensor $\gamma\dot{x}^* + n$
Time (seconds)
log of r.m.s Error
C1
C2

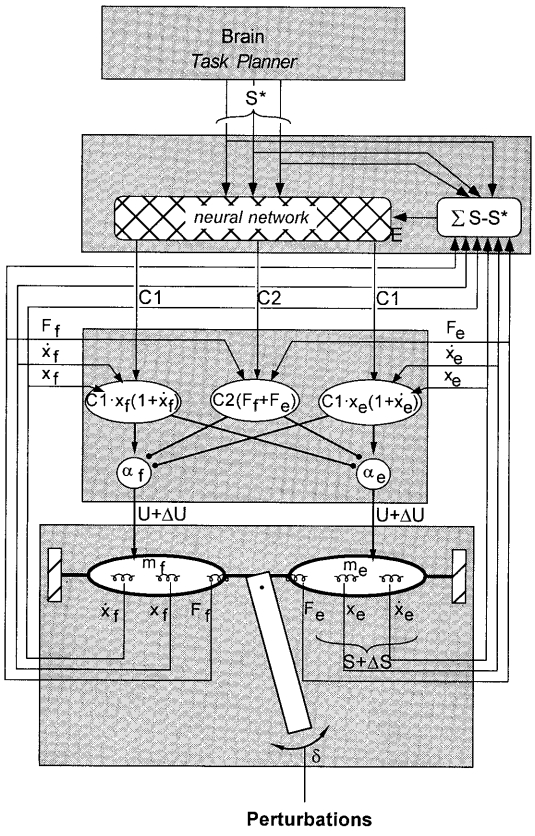

Fig. 7 Schematic design of model 3, used to test postural maintenance by a pair of antagonist muscles. *Black dots* in place of *arrows* denote inhibitory inputs to motoneurons. *Symbols* as in Figs. 1 and 5

trajectories in the unperturbed condition (compare top graphs in Fig. 6A and D).

Postural stabilization with antagonistic muscles (model 3)

Muscles and their proprioceptors usually operate in antagonist pairs through cross-connected interneurons. As shown in Fig. 7, even a single such pair introduces many more sensors, interneurons, and command signals. In order to simplify the model, we restricted it to the elements required to stabilize a mid-position posture; there were no elements that by themselves could produce movement of the joint. The muscles operated through realistically compliant tendons on an arm that presented a purely inertial load (compliant tendons are important when moving inertial loads, but were omitted for simplicity in viscoelastic models 1 and 2). The two interneurons receiving length and velocity feedback were connected in the reciprocal manner typical of muscle spindles, with excitatory output to each homonymous alpha motoneuron and inhibitory output to the antagonist alpha motoneuron (inhibition would normally be conveyed via a Ia inhibitory interneuron under separate gain control, but that was not included in this model). These two interneurons received the same *C1* command, which permitted the gain of this feedback to be varied, but prevented any asymmetry of motoneuron activation unless and until an external perturbation broke the symmetry of the sensory feedback. Similarly, the interneuron receiving the *C2* command received force signals from both muscles and distributed inhibitory feedback equally to both alpha motoneurons (in a manner similar to the non-reciprocal Ib inhibitory interneurons). Because of limited command inputs to this model, a high degree of co-contraction can only be obtained with high reciprocal reflex gain (through *C1*); the co-contraction level can then be reduced by increasing the non-reciprocal inhibitory input and negative force-feedback gain (through *C2*). The descriptions below are based on the emergent behavior of the system.

We tested the ability of this model to stabilize the arm at mid-position in the face of sinusoidal torque perturbations at different frequencies, in a manner similar to the behaving monkey experiments of Humphrey and Reed (1983). The positional error surface for 0.25-Hz torque is shown in Fig. 8A and for 5-Hz torque in Fig. 8B. Fig. 8C and D show the corresponding energy consumption in both muscles, based on a model proposed by Schutte et al. (1993), which includes the very large effect of sarcomere velocity on the economy of force production (see Appendix for details). The shapes of the error surfaces for the two frequencies of perturbation are very different, in fact almost reciprocal, despite the fact that the model system and the behavioral task (stabilize the arm at mid-position) were the same. To understand these differences, we picked three sets of control settings for kinetic analysis (Fig. 9):

I. Moderate co-activation with low-gain length-servo, which produced excellent performance and low energy consumption at 5 Hz, but very poor regulation at 0.25 Hz.
II. Moderate co-activation with high-gain length-servo, which produced excellent performance and low energy consumption at 0.25 Hz, but very poor regulation at 5 Hz.
III. High co-activation with moderate-gain length-servo, which produced fairly good performance, but at fairly high energy cost for both perturbation frequencies.

◀ **Fig. 6** Relative performance of all command strategies for the conditions indicated in **A–D**. In each pair of plots, the *top plot* shows the spindle output signals for all trials at a command setting producing optimal performance in the most realistic condition D; the *bottom plot* shows the error of each command setting for the performance conditions given, with the *red circle* indicating the setting for the top plot. *Colors* normalized to minimal error within each condition. **A** No perturbations, no spindle noise, no clipping of spindle output. **B** Six trials with force perturbations of ±0.3 F_0×50 ms at 100, 200, or 300 ms into trajectory, no spindle noise or clipping. **C** Thirty-six trials with the same six force perturbations as in **B** times six sets of band-limited noise in the velocity-sensor (2–5 Hz, *rms amplitude bar* next to *Noisy*), no clipping. **D** Thirty-six trials as in **C** with spindle output clipped to the range of –0.4 to +0.1

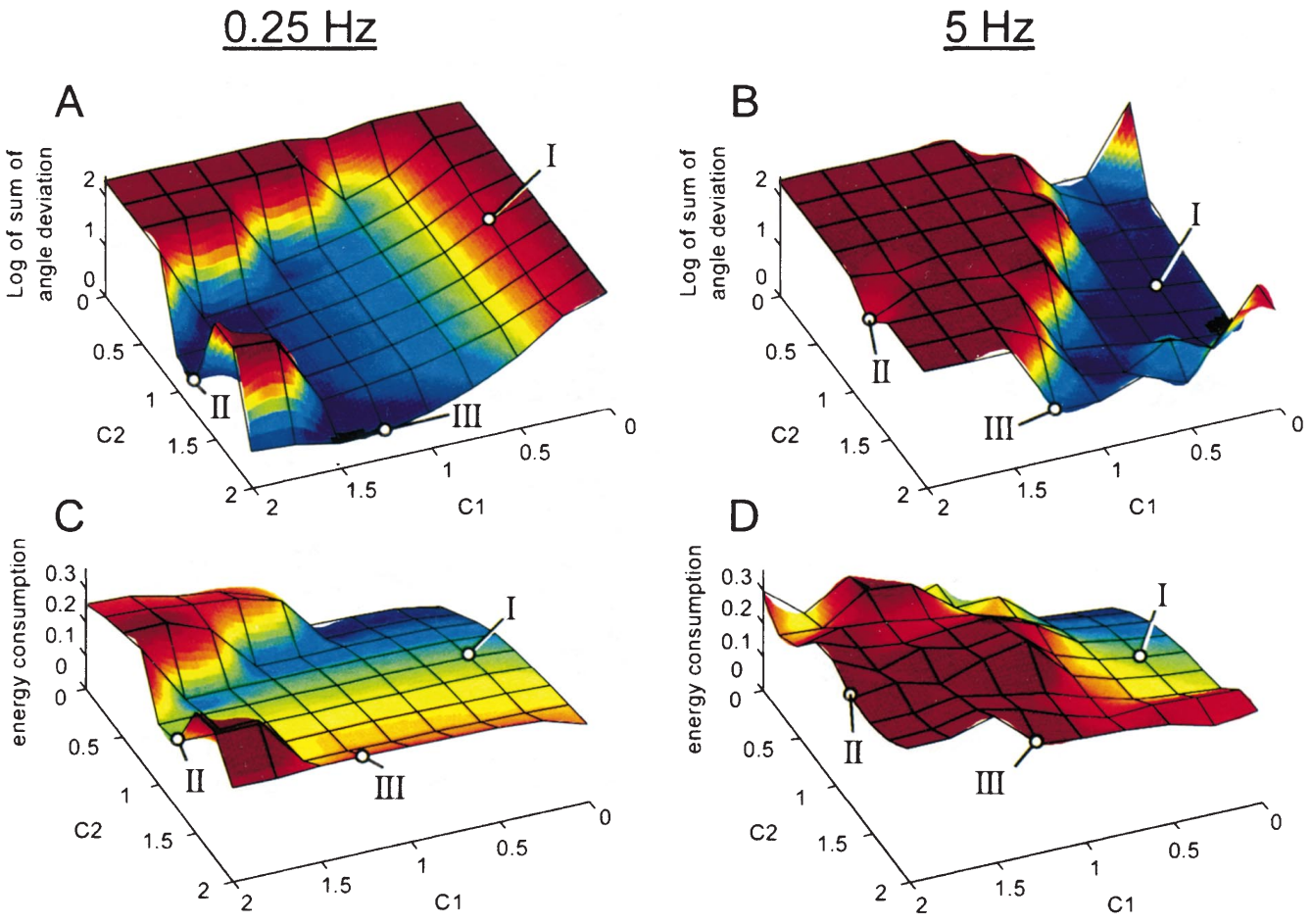

Fig. 8 Performance of model 3 for a wide range of command settings (C1, C2) during sinusoidal force perturbations at 0.25 Hz (**A**) and 5 Hz (**B**). **C, D** Corresponding plots of total energy consumption. Roman numerals (*I, II, III*) denote strategies selected for detailed analysis in Fig. 9

At low frequencies, the high-gain length-servo of strategy II provided the best trade-off between position and energy consumption when it operated just at the edge of instability. The same degree of co-activation, but with a low gain (strategy I) performed poorly because the velocity of the perturbations was too slow to produce much stabilizing force from the intrinsic properties of the muscles. Even higher co-activation (strategy III) produced a tremor-like oscillation due to the interaction of the high force and length feedback and the activation delay. For high frequency perturbations, strategy I (low gain) provided the best trade-off because the activation delays in the stretch-reflex loop were longer than a half-cycle of the torque perturbations, causing their contribution to be out-of-phase and destabilizing. Co-contraction was the only effective strategy for opposing such rapid perturbations because the intrinsic force-velocity properties of muscle are instantaneous. Its effectiveness is limited by willingness to expend energy on co-contraction and by the in-series compliance of the tendons incorporated to make this model realistic.

In one sense, all of the command states possible for model 3 are redundant in that they all maintain the arm at the desired position (centered) and velocity (zero) and they all respond to perturbations with restoring forces. Optimal strategies could be identified only when the task was further specified by including the frequency of the perturbations and by considering metabolic as well as kinematic performance criteria. When such considerations were added, the performance of this very simple system became similar to that reported in the forearm of a behaving monkey (Humphrey and Reed 1983).

Discussion

Sensitivity to model parameters

The very simple models employed in this study were selected in order to identify qualitatively their emergent behaviors rather than to simulate quantitatively the performance of any particular biological limb. The main consideration in selecting specific functions and coefficients was that the system exhibit a sufficiently wide range of stable behavior in order to assess the relative performance of the range of commands tested. In the course of developing the models described here, we experimented with a wide range of different model archi-

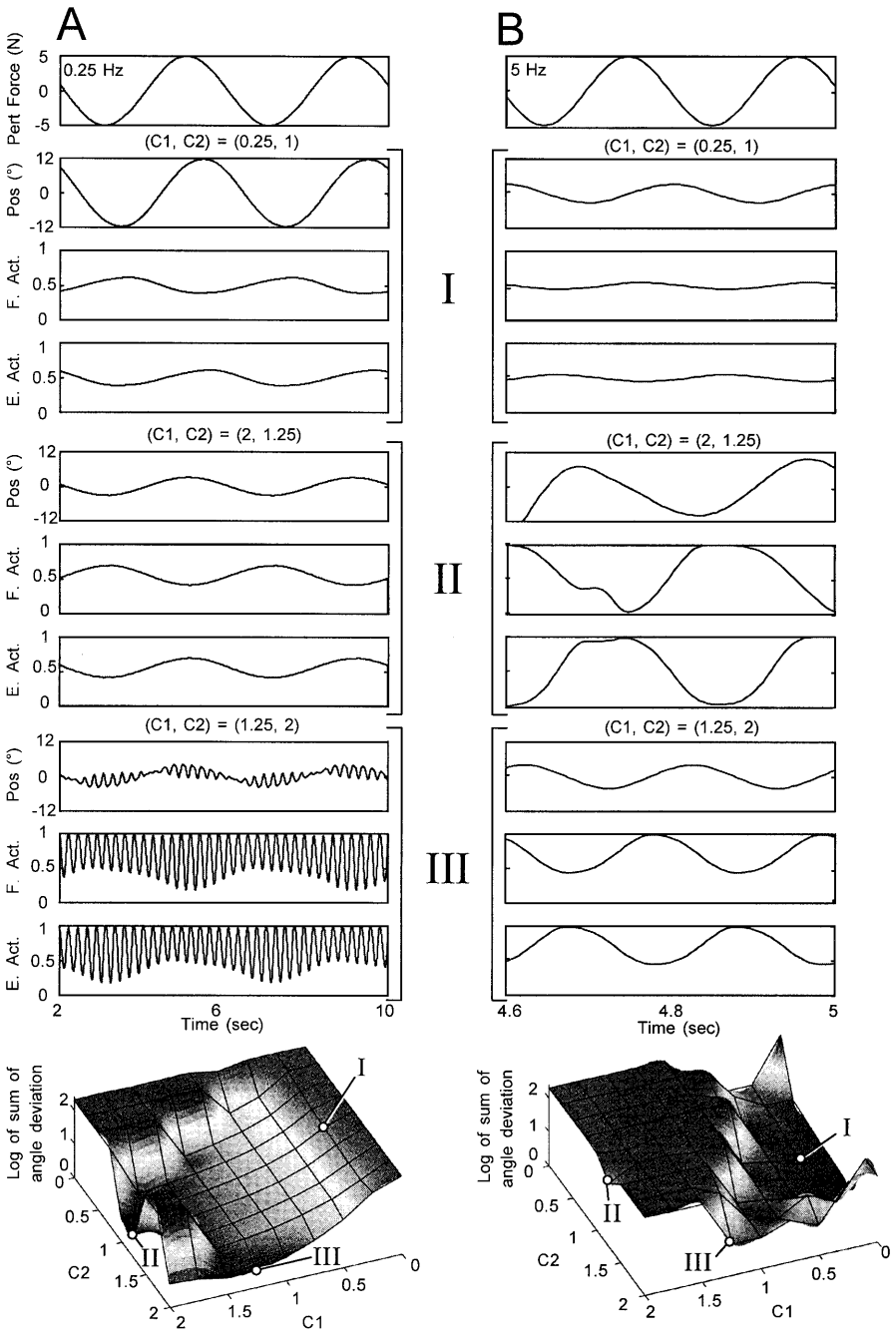

Fig. 9 Performance of model 3 versus time for the last two cycles of force perturbations at 0.25 Hz (**A**) and 5 Hz (**B**) (note different time scales), comparing strategy I (moderate co-activation with low-gain length-servo), II (moderate co-activation with high-gain length-servo), and III (high co-activation with moderate-gain length-servo). *E. Act.* Extensor muscle activation, *F. Act.* flexor muscle activation

tectures and parameters. As reported previously for somewhat more realistic model systems, it seemed to be important for interneurons to provide sufficiently rich multimodal sensory feedback (Loeb et al. 1989, 1990) and for muscle models to incorporate a realistic force-velocity relationship (Brown and Loeb 1999). Springlike restoring forces, such as used in the alpha equilibrium model of limb control (Bizzi et al. 1984), were not very effective in dealing with pulsatile force perturbations, whether they arose from the intrinsic properties of muscles or from reflexes. Details such as an additive or multiplicative relationship of the sensory signals (e.g., length plus velocity as in models 1 and 2 vs. length times velocity as in model 3 or various exponential relationships proposed previously for spindle models; Houk et al. 1981) had little effect on the qualitative performance of these models, although a multiplicative gain from the command signals was important.

Mechanisms of sensorimotor regulation

"Preflexes" – intrinsic muscle properties (model 3)

The complex intrinsic properties of muscle are at the lowest level of the hierarchy. Perturbations of length and

particularly velocity produce changes in contractile force with zero delay (as shown in Fig. A1; Brown et al. 1996). We have called these responses "preflexes" (Brown et al. 1995; Brown and Loeb 1999) because they depend on the activation level of the muscle and hence are under CNS control. The preponderance of antagonist muscle pairs in musculoskeletal architecture makes it possible for the brain to change the gain of the preflexes independently of the net torque available to produce overt movement or reaction forces in external objects. In various preparations and behaviors, preflexes appear to provide substantial and immediate responses to perturbations, which tend to stabilize the system (Humphrey and Reed 1983; Gottlieb 1994), thereby reducing the gain required in the reflexive feedback loops and reducing the instability that tends to arise when using high gains in loops with long delays (Gordon et al. 1986; Loeb et al. 1994). (Physiological systems usually include substantial nerve conduction and synaptic transmission delays as well as the muscle activation delays modeled here.) More generally, the intrinsic properties of a complete musculoskeletal system can be described as a complex impedance, including spring-like (force-length) and viscous-like (force-velocity) preflexes plus inertial (force-acceleration) terms (Hogan 1985). In a system with kinematic redundancy, the posture of the body can be used to modulate the inertial (third-order) component of impedance presented at the end-point of the limb.

"Lumpy set" of spinal interneurons (models 1, 2, and 3)

Over the past thirty years, more and more of the spinal interneurons have been identified and their various inputs and outputs characterized (McCrea 1986; Jankowska 1992). While many classes of interneurons probably remain to be discovered, certain patterns and roles are becoming clear. Spinal interneurons generally receive some combination of descending and sensory input and project directly or indirectly to diverse motor nuclei. The sensory input usually arises from a range of modalities and sources, but it is clearly neither random nor are all possible combinations represented. In developing the model system for the simulations presented here, it was apparent that the controllability of a particular musculoskeletal plant in a particular task depended on the availability of a set of interneurons with reasonable connectivity. Spinal regulators composed of poorly chosen interneurons may produce only inadequate or unstable control programs, regardless of gains (Loeb et al. 1989). Changing the conditions for which a given task was optimized often resulted in a similar nominal activation of the motoneurons in the absence of perturbations (U), but a very different distribution of activity among the available interneurons driving those motoneurons (model 3, Figs. 8 and 9). This switching function confers advantages for control that are not present in other models of motor control that are based on convergence of commands and feedback on a single type of interneuron, such as the lambda model of the equilibrium-point hypothesis (Feldman and Levin 1994). Such advantages have been noted before (Bullock and Contreras-Vidal 1993), but those models have not explained how the brain learns to achieve them.

The same spinal interneurons that produce nominal motoneuronal activity (U) also produce reflex activity (ΔU) both in our model and in physiological systems. Unlike our linear model, however, ΔU in real organisms may differ qualitatively as well as quantitatively from U. This is because real neurons have nonlinear threshold properties. By selectively polarizing various inactive motoneurons or interneurons near or far from threshold, the controller can program the regulator to eliminate some reflexes (Horak and Diener 1994) or to produce patterns of net reflex muscle activation that are very different from those that occur in the absence of perturbations (e.g., short-latency non-autogenic reflexes; Cole et al. 1984; Cole and Abbs 1987). This seems to be particularly true for cutaneous inputs, which often trigger complex responses that are not simply scaled up versions of the ongoing motor program and which may be learned rather than genetically specified (Loeb 1993). These contingency responses may be quite different from the simple reflexes that necessarily arise from the convergence of sensory signals on interneurons that are nominally active.

The various classes of interneurons that have evolved in the spinal cord probably reflect something about general principles of control in mechanical systems as well as the particular musculoskeletal linkages of the species in question. The interneurons employed in our models are most like the propriospinal interneurons (Jankowska et al. 1973; Lundberg 1992). The roles and relative importance of such interneurons for voluntary movements of the limbs have been well demonstrated (e.g., Alstermark et al. 1986; Nielsen et al. 1995; Pierrot-Deseilligny 1996). The relatively recent phylogenetic development of direct corticomotoneuronal connections (Maier et al. 1997) offers a way to bypass the limitations of the preexisting interneuronal system when entirely new behaviors are required, such as in fine control of the digits and the vocal tract in primates.

Fusimotor program (model 2)

The fusimotor-afferent-motoneuron loop has been interpreted in terms of its potential contribution to observed patterns of muscle recruitment, either by assuming fixed patterns of alpha-gamma co-activation (Vallbo 1974; Marsden et al. 1976) or more complex schemes (Bullock and Grossberg 1992; Bullock and Contreras-Vidal 1993). Muscle spindles, however, provide the main source of feedback about posture and movement to many different parts of the CNS (Gandevia et al. 1990; Gandevia 1996). Their importance appears to be reflected in their distributions (Scott and Loeb 1994), specializations (Richmond et al. 1986), and powerful and continuous modulation of their sensitivity via several distinct types of fusi-

motor control (Schieber and Thach 1980; Loeb 1984; Prochazka et al. 1989). Different motor tasks are accompanied by distinct fusimotor programs (Prochazka et al. 1988), which tune the receptors to the type and range of mechanical input expected during each task (Schieber and Thach 1980; Loeb 1984; Loeb and Marks 1985; Scott and Loeb 1994). This raises the question of how such programs are computed and implemented.

While some brainstem centers have been found that exert preferential control over the various aspects of length and velocity sensitivity of mammalian spindles (Jeneskog and Johansson 1977), there is little evidence that the descending control pathways are hardwired for separate control of gamma versus alpha motoneurons. Furthermore, beta motoneurons that innervate both intrafusal and extrafusal muscle fibers are numerous in certain mammalian muscles (Barker et al. 1977) and predominate in submammalian species. In the model presented here, the fusimotor program is simply an emergent property of a global optimization of performance, operating through a well-designed set of spinal interneurons, at least some of which have selective effects on fusimotor neurons. In order for the emergent fusimotor program to approximate the optimal information solution for the sensor, it is necessary to include the effects of both noise and limited dynamic range in the model of the sensor, as shown in Fig. 6D. The effects on performance are actually fairly subtle, both in our model (Fig. 6) and in reality (Loeb and Hoffer 1985). These effects are well-known, but have generally been treated as side-effects that simply degrade performance rather than fundamental determinants of emergent behavior in sensorimotor systems.

Specification of motor tasks

Extrinsic versus intrinsic coordinate frames

In the brain itself, some coordinate transformations must occur between relatively orthogonal representations of the outside world (e.g., visual space) and the intrinsic coordinates of the somatosensory receptors and the spinal interneurons, but little is known about where these might be computed. In our model of the task planner, we found it possible, indeed highly useful, to describe motor tasks and even external loads (see below) in the intrinsic coordinate frame of the somatosensory receptors. For a visually directed reaching movement, for example, there would be a direct conversion from the extrapersonal coordinate frame of the visual system to the set of proprioceptive signals associated with positioning the limb at that location in space. This is not inconsistent with summaries of neural activity in higher centers, such as motor cortex, that have been computed in Cartesian extrapersonal space coordinates representing the distal end of the limb (Georgopoulos 1995). The process of computing population vectors from neural activity data is a form of curve-fitting that works equally well in any complete coordinate space (Mussa-Ivaldi 1988; Sanger 1994). The use of an "over-complete" coordinate system, such as naturally occurring proprioceptors, is actually advantageous in that it represents changes in neural activity that occur when the same hand movements are made in different arm postures (Scott and Kalaska 1995), whereas vectors in end-point coordinates cannot represent such changes (Georgopoulos 1995).

Load versus perturbation

The use of the intrinsic coordinate system of the sensors for planning motor tasks presents an interesting opportunity for identifying and adjusting for loads in a simple way, a particularly vexing problem in robotics (Atkeson et al. 1986). The sensors available in Fig. 1B include all of the state variables (force, length, and velocity) necessary to describe completely any load consisting of spring-like and dashpot-like properties. Thus, when the task planner requests a particular trajectory or target in terms of these sensory signals, it is implicitly making a hypothesis about the load – if the surface of states possible with that load does not intersect the target, then no controller output can ever reach that target. Note that there is no distinction between the intrinsic load of the limb itself and external loads added to that limb. Note also that any complete set of sensory modalities could be used, including those that are non-orthogonal (e.g., a pure length sensor like the spindle secondary afferent plus a combined length and velocity sensor more like the spindle primary afferent) or those that have no simple relationship to traditional state variables such as force, length, and velocity. (Characterization of inertial load requires information about acceleration, which is probably computed from force, pressure, and velocity over time rather than sensed directly.) Representing load in whatever intrinsic sensory coordinates are available avoids the computationally intensive conversion of sensory data into load-centered descriptions such as mass, inertia, and compliance and then the further conversion into the body-centered representations normally required to plan manipulation of loads by robotic controllers.

In the simulations presented here, the target always lay on the achievable surface in the multidimensional sensory space *S*. Random perturbations caused random, but symmetrically distributed deviations between actual sensory feedback *S* and desired feedback *S**, which the controller attempted to minimize by selecting the optimal command signals. Any persistently nonrandom error would be interpreted in our system as the cue to change the estimate of load. This might account for the well-known "hefting behavior" of subjects asked to characterize the inertial properties of an unknown object in order to decide how to manipulate the object (Klatzky and Lederman 1993). The subject makes an estimate of the load based on visual appearance and selects a target trajectory in a well-practiced part of space *S*. The behavior is then repeated several times rather than only once; in our mod-

el system, this is necessary to distinguish the effects of a random perturbation from a persistent error in load-estimation, both of which result in nonzero S-S^*.

Over-complete systems versus underspecified tasks

In the absence of perturbations, all three of the models presented here could have been described as over-complete in that they produced similar performance for a broad range of different command signals. Various attempts have been made to solve "redundancy problems" by postulating the existence of rules in the central nervous system, whereby otherwise equivalent control strategies are automatically ranked according to internal criteria that are not obvious from the specification of the task itself. Examples include minimizing total muscle activation, force, or energy consumption, or maximizing straightness or smoothness of trajectory (Davy and Audu 1987; Collins 1995). In our models, the addition of perturbations to the task resolves the redundancy without adding performance criteria beyond the original kinematic target (see also Brown and Loeb 1999). Recently, Sabes et al. (1998) analyzed trajectories in a three-dimensional pointing task around an obstacle and identified just such an implicit strategy; the preferred trajectories adopted by subjects took advantage of the inertial properties of the arm to minimize the possibility that random, internally generated perturbations in their motor output would cause collision with the obstacle. All of this suggests that at least some of the motor invariances that have been described in the motor psychophysical literature may emerge from implicit constraints buried in the task or the lower levels of the neuromuscular system rather than from computational strategies of the brain.

As the number of elements increases, there are likely to be more local minima in the kinematic control space. In principle, these can be resolved by appeals to kinetic and metabolic parameters, such as the energy consumption used, to distinguish the local minima in Fig. 8 (although in practice, they may remain matters of individual habit or style). One powerful mechanism contained within our model, but unexplored in these simulations is the use of the weighting coefficients (W) that are part of the specification of the target. These change the relative contributions of various sensory modalities to the error signal that is minimized by the adaptive controller. By setting Ws appropriately, the task planner can cause the adaptive controller to settle on command strategies that optimize particular performance criteria such as speed, effort, or force or positional error with respect to the target (Stein 1982). Thus, the general form of the model is suitable for exploring a wide range of classical motor psychophysical phenomena. It should also be noted that more realistic models could incorporate time-varying command templates to control explicitly the trajectory as well as the end-point of tasks, for example to produce movement around an obstacle.

Implications for experimental design

One general prediction of these hierarchical models is that tasks that appear to be similar under nominal conditions will be performed using quite different control strategies if the subject perceives a change in the probability that particular perturbations will occur during the tasks. These control strategies may manifest themselves as different distributions of EMG activity in various muscles during unperturbed trials and in the gain of various reflexes elicited when a perturbation actually occurs; both types of strategy have been observed in human subjects performing a pseudorandomly perturbed pointing task (Jiang, Kim, Lee and Loeb, unpublished data from experiments in progress). Note that the critical factor is the perception of the subject rather than the actual occurrence of perturbations. This makes it possible to study the performance of the task with and without various perturbations as long as the overall probability distribution does not change sufficiently to be noticed. Conversely, if the behavioral strategy selected by a subject depends on his or her perception of the probability of occurrence of external and internal perturbations or the need to avoid fatigue, then we must be careful to design behavioral experiments in which the subject is in a predictable steady-state regarding the expectation and consequences of perturbations, both those applied externally by the experimenter and those likely to be generated by the subject's own neuromuscular apparatus.

Appendix

Muscle model

The muscle model had identical initial parameters in each of the three simulations. An automated script for generating scaled muscle models with these properties is described under model 3.

- L_0 (peak of tetanic force/length relationship) 10 cm
- F_0 (tetanic isometric force at L_0) 600 N
- mass of muscle 0.25 kg
- L_0^T (model 3 only) 15 cm

We used a Hill-type muscle model (Hill 1938) with a contractile element and parallel passive elastic element. A series-elastic tendon was incorporated into model 3 only (for parameters, see Fig. A4). The equations and constants for all musculotendon components were taken from Brown et al. (1996), which is based on an experimental study of the slow-twitch feline soleus muscle (Scott et al. 1996). The general properties of the muscle model are illustrated graphically in Fig. A1.

Activation filter

In order to simulate the excitation-contraction delay, a filter was interposed between the motoneuron excitation (u) and the muscle activation that drives the muscle

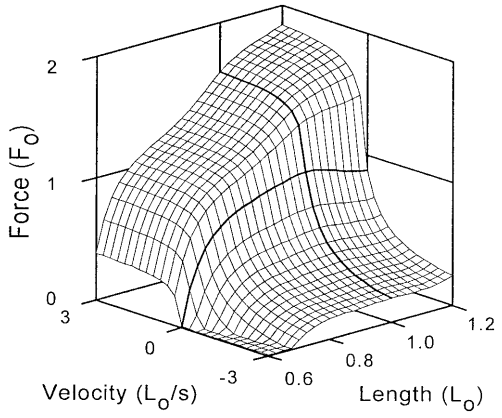

Fig. A1 For a constant level of muscle activation (in this case, maximal tetanic), the force output (*vertical axis*) depends on both the length and velocity of the sarcomeres. Note particularly the steep and discontinuous slope on either side of zero velocity (isometric), which results in large and instantaneous changes in force output in response to external perturbations. Adapted from (Brown et al. 1996)

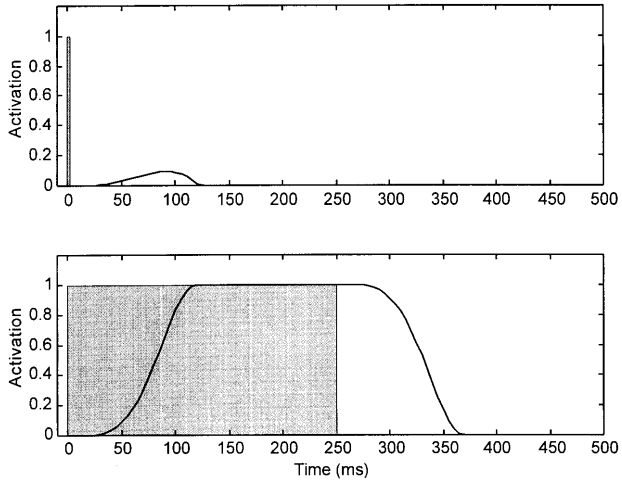

Fig. A2 The *hatched areas* represent the motoneuron excitation (impulse in *top graph*, train in *bottom graph*), while the *unshaded curves* represent the muscle activation after the excitation has been filtered. Two different durations of motoneuron excitation and their resultant muscle activations are depicted

model. The filter delays the activation 15 ms and spreads it over the next 105 ms, so that the effects of any neural input last a maximum of 120 ms. The digital filter is described by the following equations:

$$act(n) = \frac{\sum_{i=M}^{N} b_i * u_a(n-i)}{\sum_{i=M}^{N} b_i},\ M = \frac{15}{T},\ N = \frac{120}{T}$$

$$b_i = \sin\left[\left(1.75 * \frac{(i-M)*T}{105}\right)^2\right]$$

where *act* is the muscle activation, u_α the motoneuron excitation, *n* the simulation frame number, and *T* the simulation frame period (in ms).

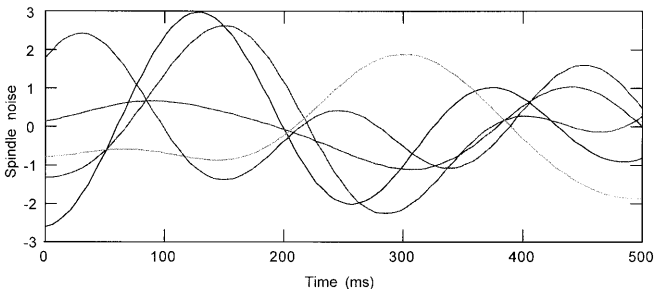

Fig. A3 Spindle-noise waveforms used in model 2

As shown in the Fig. A2, the step response of this leaky integrator produces realistically fast rise and slow decay times, although its impulse response is actually the reverse. For the conditions under which this model was used (step increases in command inputs with relatively gradual modulation by sensory feedback), the unphysiological impulse response has a relatively small effect.

Model 1 (single-muscle model)

The single muscle acted directly on a massless load, which was modeled as the sum of one velocity-dependent element (nonlinear viscosity) and one length-dependent element (nonlinear spring):

$$Load\ (L,V) = (L - L_0)^2 + \frac{V + sign(V) * \sqrt{|V|}}{5}$$

Excitation of the motoneuron depended on two interneurons, one force- and length-sensitive and the other velocity- and length-sensitive; the sum was clipped between 0–1. Lengths were biased to 0.5 L_0:

$$u_a(L,V,F) = C1 * [(L - 0.5) - F] + C2 * \left[(L - 0.5) + \frac{V}{2}\right]$$

The *C1* and *C2* terms represent command inputs to the respective interneurons, which were simulated for all combinations from 0 to 1, with steps of 0.1. The set of 12 perturbations included magnitudes of –0.2, –0.1, +0.1, and +0.2 F_0, duration of 50 ms, applied at either 100, 200, or 300 ms after onset of the command inputs to the interneurons.

Model 2 (fusimotor model)

The muscle and load models were the same as in model 1. Motoneuron excitations were defined as:

$$u_\gamma = C1 * (L - 0.5)$$

$$u_\alpha(L,V) = C1 * (L - 0.5) + C2 * \left\{(L - 0.5) + W_V\left[\left(V - V_{target}\right) * u_\gamma + noise\right]\right\}$$

where W_V is the spindle-velocity weighting, chosen to be 2.5; V_{target} the target-velocity bias, chosen to be –0.32 L_0/s; and *noise* the noise value.

The range of inputs to the interneurons and the set of perturbations were the same as in model 1. Six different

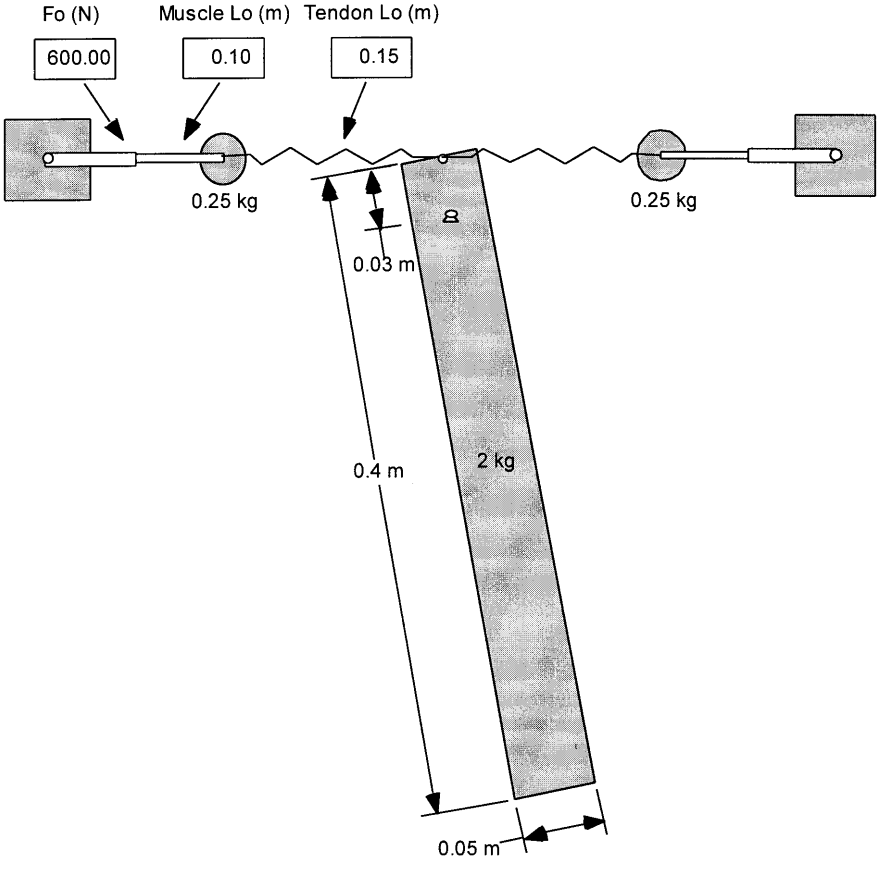

Fig. A4 The parameters in the *boxes* are input variables to a script that creates a scaled musculotendon component in the Working Model with properties described in Brown et al. (1996) (see Fig. A1) and used throughout this study. This script and information on how to use it are available on the Internet at http://brain.phgy.queensu.ca/muscle_model

spindle-noise waveforms (Fig. A3) were generated by summing 101 sine waves distributed evenly between 2 and 5 Hz with random time delays:

$$noise(t) = \sum_{i=0}^{100} \sin\left[2\pi\left(\frac{3}{100}i + 2\right) * (t - rand)\right] * 0.015\, L_0 / s$$

where *rand* is a random number between 0 and 1.

Model 3 (two-muscle model)

The musculoskeletal parameters are shown schematically in Fig. A4, which depicts the graphical user interface of the Working Model 2D 4.0.1 software (Knowledge Revolution, San Mateo, Calif., USA). Note the incorporation of a series elastic element based on equations and constants from Brown et al. (1996).

Each muscle had an independent neuron governing the activation of that muscle. The activation was dependent on the force, length, and velocity of the muscle. The equation for activation level of the flexor is given below. The same equation was used for extensor activation, but with any terms referring to the extensor switched to refer to the flexor and vice-versa:

$$u_{act}(flexor) = C1 * \left[\left(L_f - 0.5\right) * \left(C_L + C_V * V_f\right) - \left(L_e - 0.5\right) * \left(C_L + C_V * V_e\right)\right] + C2 * \left(1 - \frac{F_{SE_f} + F_{SE_e}}{2}\right)$$

where C_L is the length-weighting factor, chosen to be 4, and C_V is the velocity-weighting factor, chosen to be 0.5. In this simulation, *C1* and *C2* values varied between 0 and 2, with steps of 0.25.

The perturbation was a sinusoidal torque, with an initial delay before applying the perturbation where the torque was 0:

$$\tau_{perturbation}(t) = c_\tau * \sin\left[2\pi * \left(t - t_{delay}\right) * freq\right]$$

where c_τ is the perturbation-torque constant, chosen to be 5 Nm; t_{delay} the initial delay before perturbation starts, chosen to be 0.1 s; and *freq* the frequency of perturbation, chosen to be either 0.25 or 5 Hz.

The energy consumed by the two muscles is based on the mechanical power generated by the muscles and the heat generated by the muscles (equations and constants from Schutte 1992; Schutte et al. 1993). The heat generated is based on the sum of the maintenance heat and the heat generated by shortening and lengthening of the muscle:

$$E = P_m + h;\ P_m = -F * V$$

$$h = \left(0.7c_h\, fl(L) + 0.3c_h\right) * act * R + \begin{cases} -\alpha * V * FL(L) * act * R, & when\ V \le 0.204 \\ (0.35V - 0.035)\, fl(L) * act * R, & otherwise \end{cases}$$

where c_h is a constant, determined to be 0.07 (Schutte 1992); *FL(L)* the normalized force-length curve; *act* the muscle activation; *R* the recovery heat constant, deter-

mined to be 2.5 (Schutte 1992); α a constant, determined to be $0.16+0.18F_{active}(muscle)$ (Schutte et al. 1993); and V the velocity of the muscle in terms of L_0/s.

Acknowledgements This research was supported by the Canadian Medical Research Council Group in Sensory-Motor Neuroscience. The authors thank their colleagues for many helpful suggestions.

References

Alstermark B, Gorska T, Johannisson T, Lundberg A (1986) Hypermetria in forelimb target-reaching after interruption of the inhibitory pathway from forelimb afferents to C3–C4 propriospinal neurons. Neurosci Res 3:457–461

Athans M, Falb PL (1969) Optimal control. McGraw Hill, New York

Atkeson CG, An CH, Hollerbach JM (1986) Estimation of inertial parameters of manipulator loads and links. Int J Robot Res 5:101–119

Barker D, Emonet-Denand F, Harker DW, Jami L, Laporte Y (1977) Types of intra- and extrafusal muscle fibre innervated by dynamic skeleto-fusimotor axons in cat peroneus brevis and tenuissimus muscles, as determined by the glycogen-depletion method. J Physiol 266:713–726

Bernstein N (1967) The coordination and regulation of movement. Pergamon, New York

Bizzi E, Accornero N, Chapple W, Hogan N (1984) Posture control and trajectory formation during arm movement. J Neurosci 4:2738–2744

Brown IE, Loeb GE (1999) A reductionist approach to creating and using neuromusculoskeletal models. In: Winters J, Crago P (eds) Biomechanics and neural control of movement. Springer, New York (in press)

Brown IE, Scott SH, Loeb GE (1995) "Preflexes" – programmable, high-gain, zero-delay intrinsic responses of perturbed musculoskeletal systems. Soc Neurosci Abstr 21:562.9

Brown IE, Scott SH, Loeb GE (1996) Mechanics of feline soleus. II. Design and validation of a mathematical model. J Muscle Res Cell Motil 17:219–232

Bullock D, Contreras-Vidal JL (1993) How spinal neural networks reduce discrepancies between motor intention and motor realization. In: Newell KM, Corcos DM (eds) Variability and motor control. Human Kinetics Press, Champaign, Ill, pp 183–221

Bullock D, Grossberg S (1992) Emergence of tri-phasic muscle activation from the nonlinear interactions of central and spinal neural network circuits. Hum Mov Sci 11:157–167

Buneo CA, Boline J, Soechting JF, Poppele RE (1995) On the form of the internal model for reaching. Exp Brain Res 104: 467–479

Burgess PR (1992) Equilibrium points and sensory templates. Behav Brain Sci 15:720–722

Burnod Y, Grandguillaume P, Otto I, Ferraina S, Johnson PB, Caminiti R (1992) Visuomotor transformations underlying arm movements toward visual targets: a neural network model of cerebral cortical operations. J Neurosci 12:1435–1453

Cole KJ, Abbs JH (1987) Kinematic and electromyographic responses to perturbation of a rapid grasp. J Neurophysiol 57:1498–1510

Cole KJ, Gracco VL, Abbs JH (1984) Autogenic and nonautogenic sensorimotor actions in the control of multiarticulate hand movements. Exp Brain Res 56:582–585

Collins JJ (1995) The redundant nature of locomotor optimization laws. J Biomech 28:251–267

Davy DT, Audu ML (1987) A dynamic optimization technique for predicting muscle forces in the swing phase of gait. J Biomech 20:187–201

Feldman AG, Levin MF (1994) Positional frames of reference in motor control. The origin and use. Behav Brain Sci

Fetz EE, Shupe LE (1990) Neural network models of the primate motor system. In: Echmilles R (ed) Advanced neural computers. Elsevier/North Holland Press, Amsterdam New York, pp 43-50

Gandevia SC (1996) Kinesthesia: roles for afferent signals and motor commands. In: Rowell LB, Shepherd JT (eds) Handbook of physiology, section 12. Oxford University Press, London, pp 128–172

Gandevia SC, Macefield G, Burke D, McKenzie DK (1990) Voluntary activation of human motor axons in the absence of muscle afferent feedback. Brain 113:1563–1581

Georgopoulos AP (1995) Current issues in directional motor control. Trends Neurosci 18:506–510

Gordon T, Stein RB, Thomas CK (1986) Innervation and function of hind-limb muscles in the cat after cross-union of the tibial and peroneal nerves. J Physiol 374:429–441

Gottlieb GL (1994) The generation of the efferent command and the importance of joint compliance in fast elbow movements. Exp Brain Res 97:545–550

He J, Levine WS, Loeb GE (1991) Feedback gains for correcting small perturbations to standing posture. IEEE Trans Autom Contr 36:322–332

Hill AV (1938) The heat of shortening and the dynamic constants of muscle. Proc R Soc Lond B Biol Sci 126:136–195

Hogan N (1985) The mechanics of multi-joint posture and movement control. Biol Cybern 52:315–331

Hollerbach JM, Atkeson CG (1987) Deducing planning variables from experimental arm trajectories: pitfalls and possibilities. Biol Cybern 56:279–292

Horak FB, Diener HC (1994) Cerebellar control of postural scaling and central set in stance. J Neurophysiol 72:479–493

Houk JC (1979) Regulation of stiffness by skeletomotor reflexes. Annu Rev Physiol 41:99–114

Houk JC, Rymer WZ, Crago PE (1981) Dependence of dynamic response of spindle receptors on muscle length and velocity. J Neurophysiol 46:143–166

Humphrey DR, Reed DJ (1983) Separate cortical systems for control of joint movement and joint stiffness: reciprocal activation and coactivation of antagonist muscles. In: Desmedt JE (ed) Motor control mechanisms in health and disease. Raven Press, New York, pp 347–372

Imamizu H, Uno Y, Kawato M (1995) Internal representations of the motor apparatus: implications from generalization in visuomotor learning. J Exp Psychol 21:1174–1198

Jankowska E (1992) Interneuronal relay in spinal pathways from proprioceptors. Prog Neurobiol 38:335–378

Jankowska E, McCrea DA (1983) Shared reflex pathways from Ib tendon organ afferents and Ia muscle spindle afferents in the cat. J Physiol 338:99–111

Jankowska E, Lundberg A, Stuart D (1973) Propriospinal control of last order interneurones of spinal reflex pathways in the cat. Brain Res 53:227–231

Jeneskog T, Johansson H (1977) The rubro-bulbospinal path. A descending system known to influence dynamic fusimotor neurones and its interaction with distal cutaneous afferents in the control of flexor reflex afferent pathways. Exp Brain Res 27:161–179

Klatzky RL, Lederman SJ (1993) Toward a computational model of constraint-driven exploration and haptic object identification. Perception 22:597–621

Loeb GE (1984) The control and responses of mammalian muscle spindles during normally executed motor tasks. Exerc Sport Sci Rev 12:157–204

Loeb GE (1993) The distal hindlimb musculature of the cat. I. Interanimal variability of locomotor activity and cutaneous reflexes. Exp Brain Res 96:125–140

Loeb GE, Hoffer JA (1985) The activity of spindle afferents from cat anterior thigh muscles. II. Effects of fusimotor blockade. J Neurophysiol 54:565–577

Loeb GE, Marks WB (1985) Optimal control principles for sensory transducers. In: Boyd IA, Gladden MH (eds) Proceedings of the international symposium: The Muscle Spindle. MacMillan, London, pp 409–415

Loeb GE, He J, Levine WS (1989) Spinal cord circuits: are they mirrors of musculoskeletal mechanics? J Mot Behav 21:473–491

Loeb GE, Levine WS, He J (1990) Understanding sensorimotor feedback through optimal control. Cold Spring Harb Symp Quant Biol 55:791–803

Loeb GE, He J, Levine WS (1994) The relationship between reflexive and intrinsic control of limb trajectories (abstract). Can Soc Biomech 7g–h

Lundberg A (1992) To what extent are brain commands for movements mediated by spinal interneurons? Behav Brain Sci 15: 775–776

Lundberg A, Malmgren K, Schomburg ED (1987) Reflex pathways from group II muscle afferents. 3. Secondary spindle afferents and the FRA: a new hypothesis. Exp Brain Res 65: 294–306

MacKay WA (1982) The motor system controls what it senses. Behav Brain Sci 5:557

Maier MA, Olivier E, Baker SN, Kirkwood PA, Morris T, Lemon RN (1997) Direct and indirect corticospinal control of arm and hand motoneurons in the squirrel monkey (*Saimiri sciureus*). J Neurophysiol 78:721–733

Marque P, Pierrot-Deseilligny E, Simonetta-Moreau M (1996) Evidence for excitation of the human lower limb motoneurones by group II muscle afferents. Exp Brain Res 109:357–360

Marsden CD, Merton PA, Morton HB (1976) Stretch reflex and servo action in a variety of human muscles. J Physiol 259: 531–560

Matthews PBC (1996) Relationship of firing intervals of human motor units to the trajectory of post-spike after-hyperpolarization and synaptic noise. J Physiol 492:597–628

McCrea DA (1986) Spinal cord circuitry and motor reflexes. Exerc Sport Sci Rev 14:105–141

McIntyre J, Mussa-Ivaldi FA, Bizzi E (1996) The control of stable postures in the multijoint arm. Exp Brain Res 110:248–264

Mussa-Ivaldi FA (1988) Do neurons in the motor cortex encode movement direction? An alternative hypothesis. Neurosci Lett 91:106–111

Nielsen J, Crone C, Sinkjaer T, Toft E, Hultborn H (1995) Central control of reciprocal inhibition during fictive dorsiflexion in man. Exp Brain Res 104:99–106

Pellionisz AJ (1986) Tensor network theory of the central nervous system and sensorimotor modeling. In: Palm G, Aertsen A (eds) Brain theory. Springer, Berlin Heidelberg New York, pp 121-145

Pierrot-Deseilligny E (1996) Transmission of the cortical command for human voluntary movement through cervical propriospinal premotoneurons. Prog Neurobiol 48:489–517

Prochazka A, Hulliger M, Trend P, Durmuller N (1988) Dynamic and static fusimotor set in various behavioural contexts. In: Hnik P, Soukup T, Vejsade R, Zelena J (eds) Mechanoreceptors. Plenum Publishing Corporation, pp 417–430

Prochazka A, Trend P, Hulliger M, Vincent S (1989) Ensemble proprioceptive activity in the cat step cycle: towards a representative look-up chart. Prog Brain Res 80:61–74

Richmond FJR, Bakker GJ, Bakker DA, Stacey MJ (1986) The innervation of tandem muscle spindles in the cat neck. J Comp Neurol 245:483–497

Sabes PN, Jordan MI, Wolpert DM (1998) The role of inertial sensitivity in motor planning. J Neurosci 18:5948–5957

Sanger TD (1994) Theoretical considerations for the analysis of population coding in motor cortex. Neural Comput 6:29–37

Schieber MH, Thach WT (1980) Alpha-gamma dissociation during slow tracking movements of the monkey's wrist: preliminary evidence from spinal ganglion recording. Brain Res 202:213–216

Schomburg ED (1990) Spinal sensorimotor systems and their supraspinal control. Neurosci Res 7:265–340

Schutte LM (1992) Using musculoskeletal models to explore strategies for improving performance in electrical stimulation-induced leg cycle ergometry. PhD Dissertation, Stanford University

Schutte LM, Rodgers MM, Zajac FE, Glaser RM (1993) Improving the efficacy of electrical stimulation-induced leg cycle ergometry: an analysis based on a dynamic musculoskeletal model. IEEE Trans Rehab Eng 1:109–125

Scott SH, Kalaska JF (1995) Changes in motor cortex activity during reaching movements with similar hand paths but different arm postures. J Neurophysiol 73:2563–2567

Scott SH, Loeb GE (1994) The computation of position sense from spindles in mono-and multiarticular muscles. J Neurosci 14:7529–7540

Scott SH, Brown IE, Loeb GE (1996) Mechanics of feline soleus. I. Effect of fascicle length and velocity on force output. J Muscle Res Cell Motil 17:205–218

Soechting JF, Flanders M (1992) Moving in three-dimensional space: frames of reference, vectors, and coordinate systems. Annu Rev Neurosci 15:167–191

Stein RB (1965) A theoretical analysis of neuronal variability. Biophys J 5:173–194

Stein RB (1982) What muscle variable(s) does the nervous system control in limb movements? Behav Brain Sci 5:535–577

Vallbo AB (1974) Human muscle spindle discharge during isometric voluntary contractions. Amplitude relations between spindle frequency and torque. Acta Physiol Scand 90:319–336